arXiv:1402.5049v1 [hep-ph] 20 Feb 2014

Quark production, Bose-Einstein condensates and thermalization of the quark-gluon plasma

Jean-Paul Blaizot, Bin Wu, and Li Yan

Institut de Physique Théorique, CEA Saclay, 91191, Gif-sur-Yvette Cedex, France

In this paper, we study the thermalization of gluons and N_f flavors of massless quarks and antiquarks in a spatially homogeneous system. First, two coupled transport equations for gluons and quarks (and antiquarks) are derived within the diffusion approximation of the Boltzmann equation, with only $2 \leftrightarrow 2$ processes included in the collision term. Then, these transport equations are solved numerically in order to study the thermalization of the quark-gluon plasma. At initial time, we assume that no quarks or antiquarks are present and we choose the gluon distribution in the form $f = f_0\ \theta\left(1 - \frac{p}{Q_s}\right)$ with Q_s the saturation momentum and f_0 a constant. The subsequent evolution of the system may, or may not, lead to the formation of a (transient) Bose condensate, depending on the value of f_0. In fact, we observe, depending on the value of f_0, three different patterns: (a) thermalization without gluon Bose-Einstein condensate (BEC) for $f_0 \leq f_{0t}$, (b) thermalization with transient BEC for $f_{0t} < f_0 \leq f_{0c}$, and (c) thermalization with BEC for $f_{0c} < f_0$. The values of f_{0t} and f_{0c} depend on N_f. When $f_0 \gtrsim 1 > f_{0c}$, the onset of BEC occurs at a finite time $t_c \sim \frac{1}{(\alpha_s f_0)^2}\frac{1}{Q_s}$. We also find that quark production slows down the thermalization process: the equilibration time for $N_f = 3$ is typically about 5 to 6 times longer than that for $N_f = 0$ at the same Q_s.

I. INTRODUCTION

Understanding how a dense system of gluons evolves into a thermalized quark-gluon plasma (QGP) is an important, and theoretically challenging, problem. After two colliding nuclei pass through each other in a relativistic heavy ion collision (HIC), a dense system of gluons is believed to be produced in a time scale of order $t \sim 1/Q_s$, with Q_s the saturation momentum characterizing the initial nuclear wave functions [1]. In this early stage, f_0, the occupation number of the produced gluons with $p \lesssim Q_s$, may be as large as $1/\alpha_s$, where α_s is the strong coupling constant. Under such conditions, it has been argued that a Bose-Einstein condensate (BEC) may develop during the approach to equilibrium, provided inelastic, number changing, processes do not play a too important role [2, 3]. The effect of such inelastic processes has been recently studied. It was found that, while they eventually prevent the existence of a transient BEC in the equilibrium state, they tend to amplify the growth of soft gluon modes, thereby accelerating the formation of a BEC [4]. The purpose of this paper is to study the effect of another type of inelastic processes, those involving the creation of quark-antiquark pairs.

The partons that are produced in the early stage of HIC are mostly gluons: the number of quarks and antiquarks is initially negligible compared to the large number of gluons. However, in a thermalized quark-gluon plasma, the energy density is given by

$$\epsilon = 3P = \left[16 + \frac{21}{2}N_f\right]\frac{\pi^2}{30}T^4, \tag{I.1}$$

where we have assumed non-interacting quarks and gluons, N_f flavors of massless quarks (and antiquarks), and T is the temperature. At the energies of the RHIC and LHC, one may take $N_f = 3$. In this case quarks and antiquarks carry 66% of the total energy. Therefore, the study of quark production in a dense system of gluons is obviously of great importance to fully understand the thermalization process.

In this paper, we obtain two coupled kinetic equations for both gluons and quarks (and antiquarks), using the diffusion approximation of the Boltzmann equation[5]. The collision term contains all the $2 \leftrightarrow 2$ scatterings between quarks and gluons, but only those $2 \leftrightarrow 2$ scatterings, with the exclusion of, for instance, inelastic $2 \leftrightarrow 3$ processes. We assume the dominance of small angle scatterings which justifies the diffusion approximation. The baryon number density is assumed to be zero. As a result quarks and antiquarks are described by

the same transport equation, which is coupled to that for gluons. These transport equations are solved numerically to study the thermalization of the quark-gluon plasma.

The present study complements that carried out in Ref. [3] where quark production was ignored. As in [3], the discussion relies on the Boltzmann equation in the small angle approximation[3, 6, 7], and both quarks and gluons are taken to be massless. As in [3], we restrict ourselves to the study of a spatially homogeneous non-expanding system. In contrast to Ref. [3], we are able to follow, albeit approximately, the evolution of the system across the onset of BEC all the way to thermalization. This is achieved by imposing a specific boundary condition on the solution of the couple equations at zero momentum. It is shown in Ref. [3] that the formation of BEC starts in an over-populated system at a finite time t_c when the gluon distribution f becomes singular at $p = 0$. In this paper, we show that, for $t > t_c$, no solution of the transport equations exists if the total number of partons with $p > 0$ is required to be conserved. However, we find solutions by properly imposing a boundary condition that corresponds to a non-vanishing gluon flux at $p = 0$. Those solutions are used to describe the evolution of the system beyond t_c all the way to thermal equilibrium, with the number density of condensed particles being deduced from the gluon flux at $p = 0$.

Quark production decreases the total number of gluons in the system and could potentially hinder the formation of a BEC. However the $2 \leftrightarrow 2$ processes included in the Boltzmann equation conserve the total number of partons. As a result, a chemical potential develops, the same for all species of particles, related to this conserved quantity. The equilibrium state is achieved for a negative value of this chemical potential provided the initial number of gluons is not too large. We qualify this situation as under-population. If, on the contrary, the initial population of gluons is large enough, no equilibrium exists without a BEC: this is the situation of over-population, which was found to occur in the absence of quark production, and was studied in [3]. Thus quark production may delay the onset of BEC but does not prevent the occurrence of the phenomenon. In fact, because the growth of the population of soft gluon mode is a fast phenomenon, and quark production is relatively slow, one even encounters situations where a transient BEC appears in the course of the evolution to equilibrium, before being eventually suppressed when quark production takes over and eliminates the excess gluons prior to thermalization.

The paper is organized as follows. The transport equations for quarks and gluons are derived in Sec. II. In Sec. III, the parameters that characterize the thermodynamic equi-

librium are determined from the initial conditions, assuming that the total parton number is fixed. Our main results obtained by solving the transport equations for various type of initial conditions are presented in Sec. IV. We conclude in Sec. V. Appendix A gives some details about the derivation of the transport equations. In Appendix B, we present series solutions of the transport equations that are valid at small p. These are used in particular to set appropriate boundary conditions at $p = 0$.

II. TRANSPORT EQUATIONS FOR A QUARK-GLUON SYSTEM

The analysis, in the framework of kinetic theory, of the evolution of a quark-gluon system towards equilibrium relies on the possibility to describe quark and gluon degrees of freedom in terms of phase space distributions. Color and spin degrees of freedom do not play essential roles in the present discussion and they will be averaged out. We shall denote the color and spin averaged distribution function of gluons with $f(t, \mathbf{x}, \mathbf{p})$ and that of quarks with $F(t, \mathbf{x}, \mathbf{p})$ throughout this paper, except in the very few cases when a short-hand notation is needed, such as in eqs. (II.2) or (II.3).

In this section we obtain two coupled transport equations that govern the evolution of $f(t, \mathbf{x}, \mathbf{p})$ and $F(t, \mathbf{x}, \mathbf{p})$. In a thermal bath of quarks and gluons, the number density of quarks whose masses are much heavier than the temperature T is negligibly small compared to that of light quarks and gluons. We thus only consider the N_f flavors of quarks, and their antiparticles, whose masses are smaller than T, and take them to be massless for simplicity. Furthermore, we assume that the baryon number density is zero anywhere in the system, and no external forces are exerted on the partons. In this case, quarks and antiquarks have the same distribution due to the $SU(N_f)$ flavor symmetry and the charge conjugation invariance of QCD. Therefore, one only needs two coupled equations for the quark distribution F and the gluon distribution f to describe the evolution of the system.

Although the number of colors and of flavors are both commonly taken to be $N_c = N_f = 3$ in realistic phenomenological studies of heavy-ion collisions, we will keep N_c and N_f as free parameters.

A. The Boltzmann equation in the diffusion approximation

The Boltzmann equation

$$D_t f^a_{\mathbf{p}} \equiv \left(\frac{\partial}{\partial t} + \mathbf{v}\cdot\nabla_{\mathbf{x}}\right) f^a_{\mathbf{p}} = \mathcal{C}[f^a_{\mathbf{p}}]\,, \tag{II.2}$$

describes the evolution of the phase space distribution function $f^a_{\mathbf{p}}$ with the collision term $\mathcal{C}[f^a_{\mathbf{p}}]$, including all the $2 \leftrightarrow 2$ scattering processes in QCD, of the form

$$\begin{aligned}\mathcal{C}[f^a_{\mathbf{p}}] =& \frac{1}{2E_p\nu_a}\sum_{b,c,d}\frac{1}{s_{cd}}\int\frac{d^3\mathbf{p}'}{(2\pi)^3 2E_{\mathbf{p}'}}\frac{d^3\mathbf{k}}{(2\pi)^3 2E_{\mathbf{k}}}\frac{d^3\mathbf{k}'}{(2\pi)^3 2E_{\mathbf{k}'}}(2\pi)^4\delta^{(4)}(P+P'-K-K')|\mathcal{M}^{ab}_{cd}|^2 \\ &\times\left[f^c_{\mathbf{k}}f^d_{\mathbf{k}'}(1+\epsilon_a f^a_{\mathbf{p}})(1+\epsilon_b f^b_{\mathbf{p}'}) - f^a_{\mathbf{p}}f^b_{\mathbf{p}'}(1+\epsilon_c f^c_{\mathbf{k}})(1+\epsilon_d f^d_{\mathbf{k}'})\right)\Big]\,,\end{aligned} \tag{II.3}$$

where a short-hand notation $f^a_{\mathbf{p}}$ is used for the distribution function of different species with the superscript a distinguishing the different particles. Capital letters are used to denote a four-vector, *e.g.*, the four-momentum P. Correspondingly, the small and bold letter $\mathbf{p}$ is used for the three vector, while small ordinary letter p stands for its module. The symbol ϵ_a distinguishes fermions and bosons: $\epsilon_a = 1$ for bosons and $\epsilon_a = -1$ for fermions. In eq. (II.3), the color and spin degrees of freedom of incoming particles a and b, and the outgoing particles c and d, have been summed over in the squared scattering matrix element $|\mathcal{M}^{ab}_{cd}|^2$. The factor ν_a stands for the number of spin $\times$ color degrees of freedom of particle a (which is $2(N_c^2-1)$ for a gluon and $2N_c$ for a quark or an antiquark), and reflects the corresponding averaging of the initial state particle a. The factor s_{cd} is a symmetry factor: $s_{cd} = 2$ if c and d are identical particles and $s_{cd} = 1$ otherwise.

In a pure gluon system, the differential cross-section $gg \leftrightarrow gg$ diverges if the momentum transfer $\mathbf{q}$ is much smaller than the momenta of the two scattering gluons. Thus, low momentum transfer or small angle scatterings dominate, which allows us to treat the Boltzmann equation in a diffusion approximation. The kinetic equation then reduces to a Fokker-Planck equation [3, 6]

$$D_t f = -\nabla_{\mathbf{p}}\cdot\mathcal{J}, \tag{II.4}$$

where $\mathcal{J}$ is an effective current that summarizes the effect of the (small angle) collisions. This current is proportional to a logarithmically divergent integral of the form

$$\mathcal{L} \simeq \int_{q_{min}}^{q_{max}}\frac{dq}{q}\,, \tag{II.5}$$

where q_{min} is of the order of the screening mass, while q_{max} is typically of the order of the temperature [8].

In a quark-gluon system, the small angle scatterings between quarks and gluons are also important. These contribute to two currents: $\mathcal{J}_g$ for gluons and $\mathcal{J}_q$ for quarks. In addition to the effect of collisions which do not alter the nature of the colliding particles, there are equally important production processes: $q\bar{q} \leftrightarrow gg$, $qg \leftrightarrow qg$ and $\bar{q}g \leftrightarrow \bar{q}g$. These production processes of quarks (gluons) in the scattering of gluons (quarks) with other particles contribute to source terms: $\mathcal{S}_g$ for the production of gluons, and $\mathcal{S}_q$ for the production of quarks.

By tracking the dominant contributions from all the $2 \leftrightarrow 2$ scattering processes between quarks and gluons, as listed in Table I of Appendix A, we then obtain two diffusion-like equations

$$D_t f = -\nabla_{\mathbf{p}} \cdot \mathcal{J}_g + \mathcal{S}_g, \tag{II.6a}$$

$$D_t F = -\nabla_{\mathbf{p}} \cdot \mathcal{J}_q + \mathcal{S}_q, \tag{II.6b}$$

where the currents are given by

$$\mathcal{J}_g = -4\pi\alpha_s^2 N_c \mathcal{L} \left[\mathcal{I}_a \nabla_{\mathbf{p}} f + \mathcal{I}_b \frac{\mathbf{p}}{p} f(1+f)\right], \tag{II.7a}$$

$$\mathcal{J}_q = -4\pi\alpha_s^2 C_F \mathcal{L} \left[\mathcal{I}_a \nabla_{\mathbf{p}} F + \mathcal{I}_b \frac{\mathbf{p}}{p} F(1-F)\right], \tag{II.7b}$$

and the sources by

$$\mathcal{S}_g = -\frac{N_f}{C_F}\mathcal{S}_q = \frac{4\pi\alpha_s^2 C_F N_f \mathcal{L}\mathcal{I}_c}{p}\left[F(1+f) - f(1-F)\right], \tag{II.8}$$

with

$$\mathcal{I}_a = \int \frac{d^3\mathbf{p}}{(2\pi)^3}\left[N_c f(1+f) + N_f F(1-F)\right], \tag{II.9a}$$

$$\mathcal{I}_b = 2\int \frac{d^3\mathbf{p}}{(2\pi)^3}\frac{1}{p}\left(N_c f + N_f F\right), \tag{II.9b}$$

$$\mathcal{I}_c = \int \frac{d^3\mathbf{p}}{(2\pi)^3}\frac{1}{p}(f+F). \tag{II.9c}$$

Here, $C_F = (N_c^2 - 1)/(2N_c)$ is the square of the Casimir operator of the color $SU(N_c)$ group in the fundamental representation. In the following, the first and second terms on the right hand side of eqs. (II.6) respectively refer to as the diffusion and source terms.

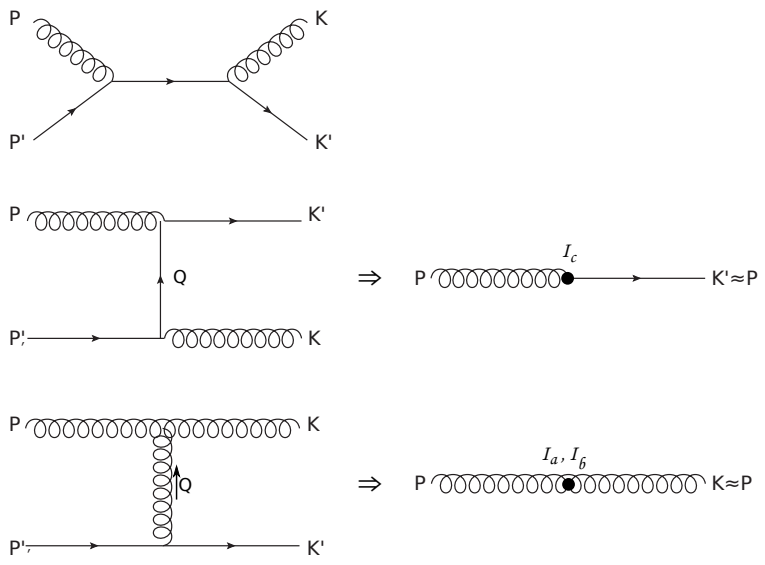

FIG. 1. Diagrams for $gq \to gq$. In the diffusion approximation, the first diagram can be neglected, the square of the second diagram contributes to the source terms S_q (and S_g) and the square of the third diagram contributes to the diffusion term with the current $\mathcal{J}_g$. The second diagram describes the decay of the gluon into a quark and its contribution to the coefficient $\mathcal{I}_c$ is given by integrating out the other partons. The third diagram describes the diffusion of the gluon in momentum space, which is controlled by the two integrals $\mathcal{I}_a$ and $\mathcal{I}_b$, which also involve integrating out the other partons.

A few comments on these new equations are in order. First, although we postpone the detailed derivations of eqs. (II.6) to Appendix A, the essential steps and concepts in these derivations can be revealed by focusing on one of the scattering processes, $gq \to gq$, for example. The corresponding diagrams are shown in Fig. 1, and the square of the associated matrix element is

$$|\mathcal{M}_{gq}^{gq}|^2/g^4 = -8N_cC_F^2\left(\frac{u}{s}+\frac{s}{u}\right)+8N_c^2C_F\frac{u^2+s^2}{t^2}\,, \tag{II.10}$$

where the Mandelstam variables are $s=(P+P')^2$, $t=(P-K)^2$ and $u=(P-K')^2$. There are two types of divergent terms in eq. (II.10) when $q \to 0$ (small angle approximation). The u channel term ($\sim 1/u$) comes from the square of the second diagram in Fig. 1, while the t channel term ($\sim 1/t^2$) comes from the square of the third diagram in Fig. 1. Substituting eq. (II.10) back into eq. (II.3), one finds that the two dominant terms are actually of the same

order in the logarithmic approximation [*]. The t channel scattering results in a part of the currents in eqs. (II.7), while the u channel contributes to the sources eq. (II.8). Repeating the same analysis for all the other $2 \leftrightarrow 2$ scattering processes, we obtain eqs. (II.6).

A second comment is that the reduced collision terms in eqs. (II.6) preserve important physical properties of the original kinetic equation, eq. (II.2). For instance, it can be verified that the equilibrium Bose-Einstein distribution for gluons and Fermi-Dirac distribution for quarks, are still the fixed point solutions to eqs. (II.6). Besides, and more importantly, the collision terms in the diffusion form conserve energy, and particle number. We provide an explicit proof for a specified case in the next section.

B. The transport equations for spatially homogeneous systems

In the following, we shall study a spatially homogeneous system of quarks and gluons. In this case the spatial dependence of the phase space distribution can be ignored and $D_t = \frac{\partial}{\partial t}$. In addition, we assume isotropy of the momentum distributions, which are then solely functions of the modulus of the momentum and of time. We introduce a new time variable

$$\tau = \frac{2\alpha_s^2 N_c \mathcal{L}}{\pi} t, \tag{II.11}$$

and denote the derivatives with respect to τ and p by overdots and primes respectively. Then eqs. (II.6a) and (II.6b) reduce to

$$\dot{f} = -\frac{1}{p^2}\left(p^2 J_g\right)' + \frac{C_F N_f}{N_c} S_g = -\frac{1}{4\pi p^2}\mathcal{F}_g' - \frac{C_F N_f}{N_c} S_q, \tag{II.12}$$

$$\dot{F} = -\frac{C_F}{N_c}\frac{1}{p^2}\left(p^2 J_q\right)' + \frac{C_F^2}{N_c} S_q = -\frac{C_F}{N_c}\frac{1}{4\pi p^2}\mathcal{F}_q' + \frac{C_F^2}{N_c} S_q\,, \tag{II.13}$$

where we have introduced the rescaled currents J_g (for gluons) and J_q (for quarks), together with the corresponding fluxes $\mathcal{F}_g$ and $\mathcal{F}_q$:

$$\frac{\mathcal{F}_g}{4\pi p^2} \equiv J_g \equiv -I_a f' - I_b f(1+f), \tag{II.14}$$

$$\frac{\mathcal{F}_q}{4\pi p^2} \equiv J_q \equiv -I_a F' - I_b F(1-F), \tag{II.15}$$

[*] Here, the difference between the medium-dependent masses of quarks and gluons is neglected, which is valid in the leading logarithmic approximation.

and the rescaled source terms

$$S_g = -S_q = \frac{I_c}{p}\left[F(1+f) - f(1-F)\right] . \tag{II.16}$$

In the equations above, the integrals I_a, I_b and I_c are defined by

$$I_a = 2\pi^2 \mathcal{I}_a = \int_0^\infty dp\, p^2 \left[N_c f(1+f) + N_f F(1-F)\right] ,$$
$$I_b = 2\pi^2 \mathcal{I}_b = 2\int_0^\infty dp\, p \left(N_c f + N_f F\right) , \qquad I_c = 2\pi^2 \mathcal{I}_c = \int_0^\infty dp\, p \left(f + F\right) . \tag{II.17}$$

Parton number density n, and energy density ϵ, are given in terms of the distribution functions f and F by

$$n = 4N_c \int \frac{d^3\mathbf{p}}{(2\pi)^3} \left(C_F f + N_f F\right) \equiv n_g + n_q, \tag{II.18}$$

$$\epsilon = 4N_c \int \frac{d^3\mathbf{p}}{(2\pi)^3} p \left(C_F f + N_f F\right) \equiv \epsilon_g + \epsilon_q. \tag{II.19}$$

In a similar manner, the entropy density of gluons s_g and of quarks s_q can be expressed in terms of f and F as

$$s_g \equiv -4N_c C_F \int \frac{d^3\mathbf{p}}{(2\pi)^3} \left[f \log f - (1+f)\log(1+f)\right] , \tag{II.20a}$$

$$s_q \equiv -4N_c N_f \int \frac{d^3\mathbf{p}}{(2\pi)^3} \left[F \log F + (1-F)\log(1-F)\right] , \tag{II.20b}$$

with the total entropy density of the quark-gluon system given by

$$s = s_g + s_q. \tag{II.21}$$

The time evolution of n, ϵ and s can be obtained from eqs. (II.12) and (II.13). The corresponding equations take the following form

$$\dot{n} = -\frac{1}{2\pi^3} C_F (N_c \mathcal{F}_g + N_f \mathcal{F}_q)\Big|_{p=0}^{p=\infty} , \tag{II.22}$$

$$\dot{\epsilon} = -\frac{1}{2\pi^3} C_F \left[p(N_c \mathcal{F}_g + N_f \mathcal{F}_q) + I_a 4\pi p^2 (N_c f + N_f F)\right]\Big|_{p=0}^{p=\infty} , \tag{II.23}$$

$$\dot{s} = \frac{C_F}{2\pi^3}\left[N_c\left(\mathcal{F}_g \log\frac{f}{1+f} - 4\pi p^2 I_b f\right) + N_f\left(\mathcal{F}_q \log\frac{F}{1-F} - 4\pi p^2 I_b F\right)\right]\Big|_{p=0}^{p=\infty}$$
$$+ \frac{2C_F}{\pi^2}\int_0^\infty dp\, p s^+(p), \tag{II.24}$$

where $s^+(p)$ is the non-negative function,

$$s^+ \equiv \frac{p}{I_a}\left(\frac{N_c J_g^2}{f(1+f)} + \frac{N_f J_q^2}{F(1-F)}\right)$$
$$+ C_F N_f I_c \left[F(1+f) - f(1-F)\right] \log\frac{F(1+f)}{f(1-F)}. \tag{II.25}$$

At this point, it is instructive to discuss the conservation of the total number of patrons and of the energy, as well as the increase of the entropy. To do so, one needs to know the behavior of f and F near $p = 0$ (the contributions as $p \to \infty$ to the time derivatives in eqs. (II.22, II.23, II.24) vanish and, therefore, can be dropped). As discussed in Appendix B, two kinds of solutions near $p = 0$ are allowed by the transport equations (II.12) and (II.13). For both types of solutions, the boundary terms on the right hand side of eqs. (II.23) and (II.24) always vanish. Therefore, $\dot{\epsilon} = 0$ and $\dot{s} \geq 0$. However, n is not conserved with both solutions. For solutions in which f and F are analytic near $p = 0$, n is conserved because $\mathcal{F}_g$ and $\mathcal{F}_q$ vanish at $p = 0$. But for solutions of the form

$$f = \frac{c_{-1}}{p} - \frac{1}{2} + \cdots , \tag{II.26}$$

$$F = \frac{1}{2} + \cdots , \tag{II.27}$$

there is a non-vanishing gluon flux $\mathcal{F}_g$ at $p = 0$

$$\mathcal{F}_g|_{p=0} = 4\pi c_{-1}(I_a - I_b c_{-1}) \quad \text{and} \quad \mathcal{F}_q|_{p=0} = 0 \, . \tag{II.28}$$

This entails a time variation of the number density

$$\dot{n} = \frac{2}{\pi^2} C_F N_c I_b c_{-1}(T^* - c_{-1}) \, , \tag{II.29}$$

where we have put

$$T^* \equiv \frac{I_a}{I_b}, \tag{II.30}$$

and the coefficient c_{-1} depends only on τ. The non-vanishing gluon flux at $p = 0$ reflects the accumulation of gluons of the zero mode, whose number density N^0 evolves according to

$$\dot{N}^0 = -\dot{n}, \tag{II.31}$$

in order to ensure the overall conservation of the parton number.

In the following, we shall follow Ref. [3] and neglect the mild time dependence of $\mathcal{L}$ in eq. (II.5). In this case eqs. (II.12) and (II.13) are invariant under the following scaling transformation

$$Q_s \to c Q_s, \quad \tau \to \frac{\tau}{c}, \quad \mathbf{p} \to c\mathbf{p} \tag{II.32}$$

with $c > 0$. As a result, one can express all momenta in units of Q_s (and the same for the chemical potential μ and the temperature T of Section III) and times in units of $1/Q_s$.

III. THERMODYNAMICS OF QGP WITH A FIXED TOTAL PARTON NUMBER

Since only $2 \leftrightarrow 2$ processes are included in the collision term of the transport equations, the total parton number is conserved. As a result, in equilibrium, gluons, quarks and antiquarks all have the same chemical potential associated to parton number conservation. The thermal equilibrium distributions are the fixed points of eqs. (II.12) and (II.13), and are of the form

$$f_{eq} = \frac{1}{e^{(p-\mu)/T} - 1}, \qquad F_{eq} = \frac{1}{e^{(p-\mu)/T} + 1}. \tag{III.33}$$

In the following T and μ will always refer to as the thermal equilibrium temperature and chemical potential.

The thermodynamic properties of such a QGP are determined by the total energy density and the total parton number density, which are respectively denoted by ϵ_0 and n_0. The under-populated and over-populated systems have very different properties[2, 3]. In an under-populated system, the values of T and $\mu < 0$ can be obtained by solving the equations

$$\epsilon_{eq} = \epsilon_0, \qquad n_{eq} = n_0, \tag{III.34}$$

where n_{eq} and ϵ_{eq} are obtained by plugging f_{eq} and F_{eq} into eqs. (II.18) and (II.19). In an over-populated system, n_0 is so large such that no real solution to the above equations exists. The thermal distributions are given by f_{eq} and F_{eq} with $\mu = 0$ and T determined from ϵ_0, i.e.,

$$T = \sqrt{\frac{2}{\pi}} \frac{(15\epsilon_0)^{1/4}}{(8N_cC_F + 7N_cN_f)^{1/4}}. \tag{III.35}$$

The excess gluons can form a BEC. The total number of partons with $p > 0$, n_{eq}, can be calculated from eq. (II.18), and the number density of the condensated gluons is given by

$$N^0 = n_0 - n_{eq}. \tag{III.36}$$

Let us take for example the system with the total energy and the particle number density

$$\epsilon_0 = \frac{f_0}{2\pi^2} N_c C_F Q_s^4, \qquad n_0 = \frac{f_0}{3\pi^2} 2N_c C_F Q_s^3, \tag{III.37}$$

as obtained from a CGC-type initial distribution

$$f(0,p) = f_0 \, \theta\left(1 - \frac{p}{Q_s}\right), \qquad F(0,p) = 0 \tag{III.38}$$

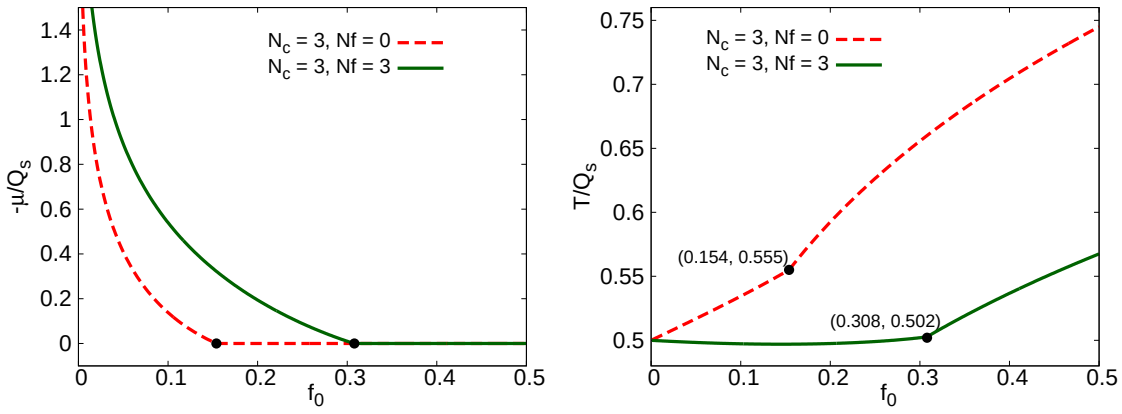

FIG. 2. The equilibrium temperature T and chemical potential μ as a function of f_0. In both figures, the transition from under-population to over-population occurs at $f_{0c} = 0.308$ for $N_f = 3$ (solid line) and $f_{0c} = 0.154$ for $N_f = 0$ (dashed line). For $f > f_{0c}$, the system is expected to be in a thermal equilibrium with vanishing μ and the excess gluons form a Bose condensate.

with $f_0 > 0$. The resulting dependence of μ and T on f_0 is shown in Fig. 2. The transition from under- to over-population happens at

$$f_{0c} = \frac{273375(4C_F + 3N_f)^4\zeta(3)^4}{2C_F(8C_F + 7N_f)^3\pi^{12}} \simeq \frac{0.309(4C_F + 3N_f)^4}{C_F(8C_F + 7N_f)^3}, \tag{III.39}$$

$$T_c = \frac{45\zeta(3)\,(4C_F + 3N_f)}{\pi^4\,(8C_F + 7N_f)}Q_s \simeq \frac{0.555\,(4C_F + 3N_f)}{(8C_F + 7N_f)}Q_s. \tag{III.40}$$

Because the production of quarks and antiquarks effectively decreases the number of gluons, larger values of f_{0c} are needed for $N_f > 0$ than for $N_f = 0$. For example, $f_{0c} = 0.308$ for $N_c = 3$ and $N_f = 3$, and $f_{0c} = 0.154$ for $N_c = 3$ and $N_f = 0$. For $f < f_{0c}$ the system is under-populated. In this case μ and T can be solved according to eq. (III.34). For $f_0 > f_{0c}$, the system becomes over-populated. The temperature is then given in eq. (III.35), that is,

$$T = \frac{1}{\pi}\left(\frac{30C_F f_0}{8C_F + 7N_f}\right)^{\frac{1}{4}} Q_s, \qquad \mu = 0. \tag{III.41}$$

The variations of the equilibrium temperature T and chemical potential μ as a function of f_0 are illustrated in Fig. 2.

IV. THERMALIZATION OF THE QUARK-GLUON PLASMA

In this section we study the thermalization of a quark-gluon system whose initial distribution is given by eq. (III.38). As discussed in the previous section, a BEC is expected to

be formed when $f_0 > f_{0c}$ while when $f_0 < f_{0c}$ there is no BEC in the equilibrium state. However, we shall show that even in the case $f_0 < f_{0c}$, when quarks are present, a BEC may appear for a short period of time due to the transient over-population of low momentum gluons. This occurs for $f_0 > f_{0t}$, where f_{0t} lies in the overlapping region between $f_{0c}|_{N_f=0}$ and $f_{0c}|_{N_f>0}$. In the following we study three different patterns of thermalization, each characterized by a specific value of f_0. In most cases, we take $N_f = 3$, in which case $f_{0t} \simeq 0.25937 < f_{0c} = 0.308$.

A. Thermalization with BEC: $f_0 > f_{0c}$

In Ref. [3], it is shown that the onset of BEC in a dense system of gluons occurs in a finite time τ_c. For the initial condition eq. (III.38), the transition value of f_0 from under-population to over-population is $f_{0c}|_{N_f=0} = 0.154$, which coincides with the value extracted from eq. (III.39) for $N_f = 0$. In this subsection, we consider the effects of the quark production on the onset of BEC and manage to follow the evolution of the system, albeit very approximately, beyond τ_c. The equilibration process is qualitatively the same for all the over-populated systems with the initial conditions (III.38). We choose $f_0 = 0.4$ and $N_f = 3$ as a specific example to show the details of how the system evolves into a thermal equilibrium state with BEC.

The formation of BEC starts at a finite time $\tau = \tau_c$ when f builds up the $1/p$ tail at small p with the coefficient[3]

$$c_{-1} = T^* = \frac{I_b}{I_a}. \tag{IV.42}$$

As discussed in Appendix B, this is easily understood from the form of the classical distribution function at small p,

$$f \simeq \frac{T^*}{p - \mu_g^*}. \tag{IV.43}$$

The onset of BEC corresponds to the effective chemical potential $\mu_g^* \to 0$, at which point $f \sim \frac{T^*}{p}$. In our numerical simulation, eq. (IV.42) is used to determine the values of τ_c[†] . The left panel of Fig. 3 shows how the effective temperature T^* keeps decreasing until it eventually approaches the equilibrium temperature T. The curve is completely smooth

[†] In our code, τ_c is calculated as the moment when $pf|_{p=p_{min}} = T^* = \frac{I_a}{I_b}$ with p_{min} the smallest momentum.

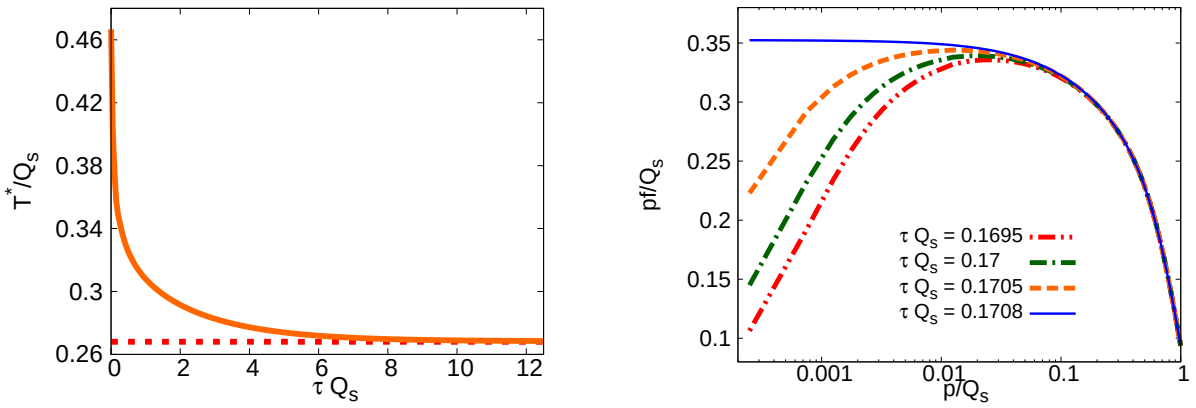

FIG. 3. The determination of τ_c. The left panel shows T^* as a function of τ, which keeps decreasing to approach the thermal equilibrium temperature $T = 0.268\ Q_s$. The right panel shows pf near τ_c, which is determined by eq. (IV.42). The dashed curves are indistinguishable from the classical thermal distribution eq. (IV.43) when $p \lesssim 0.1\ Q_s$. Here, $f_0 = 0.4$ and $N_f = 3$, and $\tau_c\ Q_s = 0.1708$.

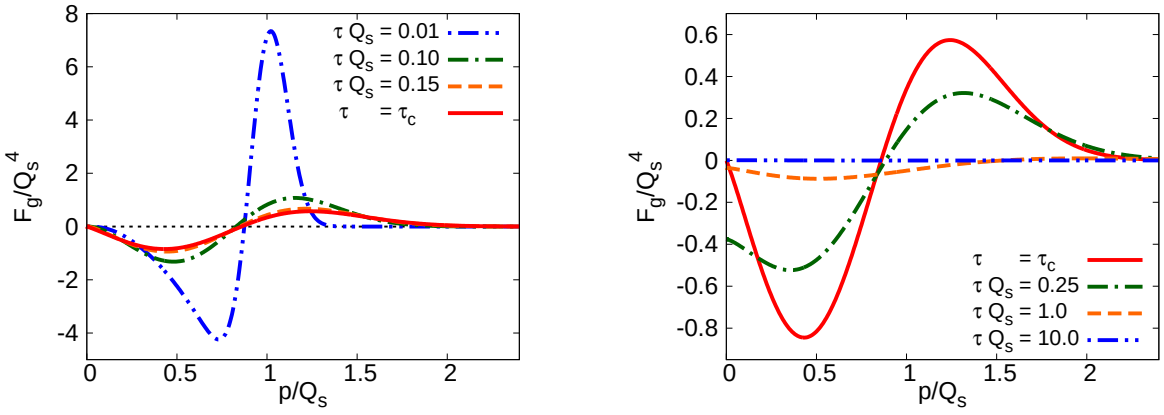

FIG. 4. The onset of gluon BEC. The gluon flux $\mathcal{F}_g$ at different times is shown as a function of p. Before $\tau_c \simeq 0.1708\ Q_s^{-1}$, $\mathcal{F}_g|_{p=0}$ vanishes (left panel). Right after τ_c, $\mathcal{F}_g|_{p=0}$ becomes finite and negative (right panel). Here, $f_0 = 0.4$ and $N_f = 3$.

and does not show any indication of the onset of BEC that occurs at $\tau_c\ Q_s = 0.1708$ (for $f_0 = 0.4$ and $N_f = 3$). The right panel of Fig. 3 shows the time evolution of f near τ_c. Before τ_c, f and F are both analytic near $p = 0$ and the gluon flux $\mathcal{F}_g$ vanishes at $p = 0$ (see the left panel of Fig. 4). That is to say, there is no accumulation of gluons at $p = 0$. At $\tau = \tau_c$, f becomes singular at $p = 0$ but the gluon flux $\mathcal{F}_g|_{p=0}$ still vanishes according

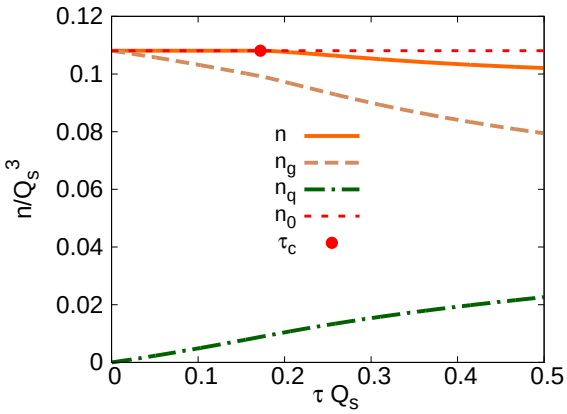

FIG. 5. Time evolution of the parton numbers around τ_c. Before τ_c, the total number of partons (with $p > 0$) n is equal to n_0. Right after τ_c, it decreases and the difference between n and n_0 is equal to the number density N_0 of gluons stored in the condensate. Here, $f_0 = 0.4$ and $N_f = 3$.

to eqs. (IV.42) and (II.28). As shown in Fig. 5, at this moment the low momentum gluons keep accumulating, as c_{-1} becomes larger than T^*. Our numerical simulation shows that after τ_c no solutions with vanishing $\mathcal{F}_g|_{p=0}$ are allowed by the transport equations in (II.12) and (II.13). As discussed in Appendix B, one can find solutions beyond τ_c by providing boundary conditions according to eq. (II.28) (or eq. (B.8)). We have used such solutions to describe the evolution of the system after τ_c. Although this procedure ignores important coupling between the condensate and the non-condensate particles, which may alter the details of the dynamics and perhaps the thermalization time scale, it has the advantage of providing a continuous transition to the correct equilibrium state. As shown in the right panel of Fig. 4 and Fig. 5, $\mathcal{F}_g|_{p=0}$ becomes negative right after τ_c, and correspondingly n starts to decreases. This reflects the formation of a BEC, with the number density of condensed gluon, N^0, increasing according to $\dot{N}^0 = -\dot{n}$.

The dependence of τ_c on f_0 can be estimated parametrically at large f_0. Since τ_c decreases as f_0 increases[3], one needs only to study the time evolution of f and F at small τ. This can be done by plugging the linear expansions

$$\begin{aligned} f &\simeq \bar{f}_0(p) + \tau \bar{f}_1(p), \\ F &\simeq \bar{F}_0(p) + \tau \bar{F}_1(p) = \tau \bar{F}_1(p), \end{aligned} \tag{IV.44}$$

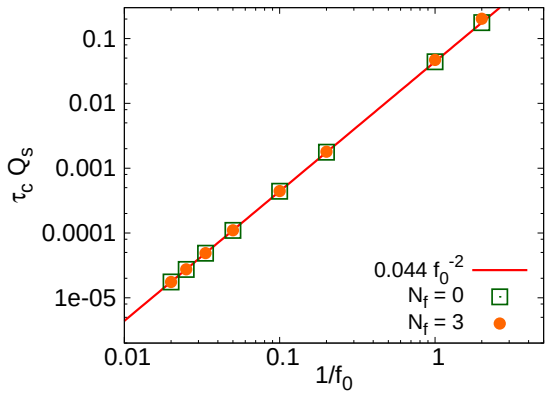

FIG. 6. τ_c as a function of $\frac{1}{f_0}$. In both cases with $N_f = 0$ and $N_f = 3$, $\tau_c \propto \frac{1}{f_0^2}$ and it is independent of N_f for $f_0 \gtrsim 1$.

into eqs. (II.12) and (II.13) and keeping terms of $O(\tau^0)$. We obtain thus

$$\bar{F}_1 = \frac{C_F^2 I_c(0)}{N_c p} \bar{f}_0, \tag{IV.45}$$

$$\bar{f}_1 = -\frac{1}{p^2}\left[p^2 J_g(0,p)\right]' - \frac{N_f C_F I_c(0)}{N_c p}\bar{f}_0, \tag{IV.46}$$

where

$$J_g(0,p) = -N_c f_0^2 (1+f_0) Q_s^2 \left[1 + \frac{Q_s}{3}\delta(p-Q_s)\right]. \tag{IV.47}$$

In the limit $f_0 \gg 1$ and $p \ll Q_s$, we have

$$\bar{f}_1 \sim \frac{2}{p}\left[I_a(0)\bar{f}_0' + I_b(0)\bar{f}_0^2\right] \sim f_0^3 \frac{Q_s^2}{p}. \tag{IV.48}$$

Here, we have dropped the term $\propto \bar{f}_0' = f_0\delta(p-Q_s)$, which vanishes at $p \ll Q_s$. Because the gluon flux vanishes at $p \sim Q_s$, f does not change significantly at $p \sim Q_s$ and one has $Q_s f(Q_s) \sim Q_s\ f_0$. Then τ_c can be estimated as the moment at which pf at small p, $f_0^3 Q_s^2 \tau_c$, just becomes comparable with pf at $p \sim Q_s$, $f_0 Q_s$, which gives

$$\tau_c \sim \frac{1}{f_0^2}\frac{1}{Q_s}. \tag{IV.49}$$

Since the quark production only contributes a term $\sim -N_f \frac{f_0^2}{p}$ to $\bar{f}_1$, eq. (IV.49) is almost independent of N_f. This parametric behavior is confirmed by our numerical results shown in Fig. 6, and it is actually valid for $f_0 \gtrsim 1$. Therefore, we conclude that the formation of BEC starts at a time

$$t_c \sim \frac{1}{(\alpha_s f_0)^2}\frac{1}{Q_s} \tag{IV.50}$$

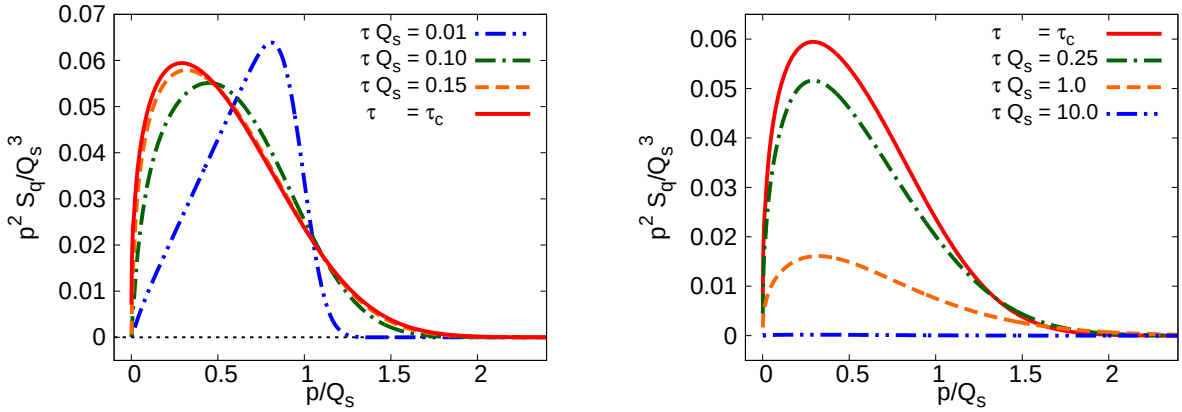

FIG. 7. Quark production. The production rate per unit momentum $p^2 S_q$ (source term multiplied by p^2) is shown as a function of p, at different times before (left panel) and after (right panel) the onset of BEC. Here, $f_0 = 0.4$ and $N_f = 3$, in which case $\tau_c \simeq 0.1708\ Q_s^{-1}$.

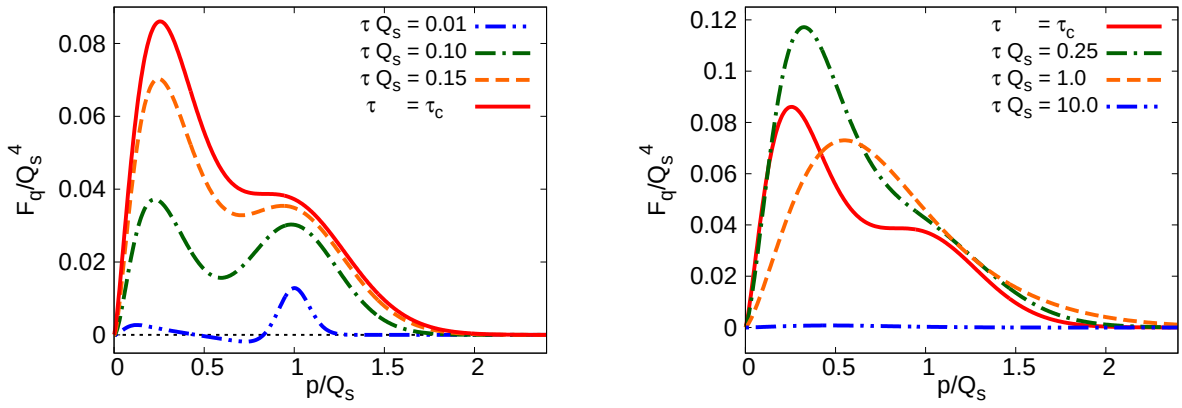

FIG. 8. The flux of the quark current as a function of momentum for different times before (left panel) and after (right panel) the onset of BEC. Here, $f_0 = 0.4$ and $N_f = 3$, in which case $\tau_c \simeq 0.1708\ Q_s^{-1}$.

for $f_0 \gtrsim 1$. Note however that for the specific value $f_0 = 0.4$ chosen for the numerical calculations presented in this subsection, $\tau_c = 0.1708\, Q_s^{-1}$.

We now consider the effect of quark production on the thermalization process. As we have already mentioned, inelastic processes involving quarks contribute both to the currents and to the source terms in eqs. (II.6). At very early times, the gluon distribution function

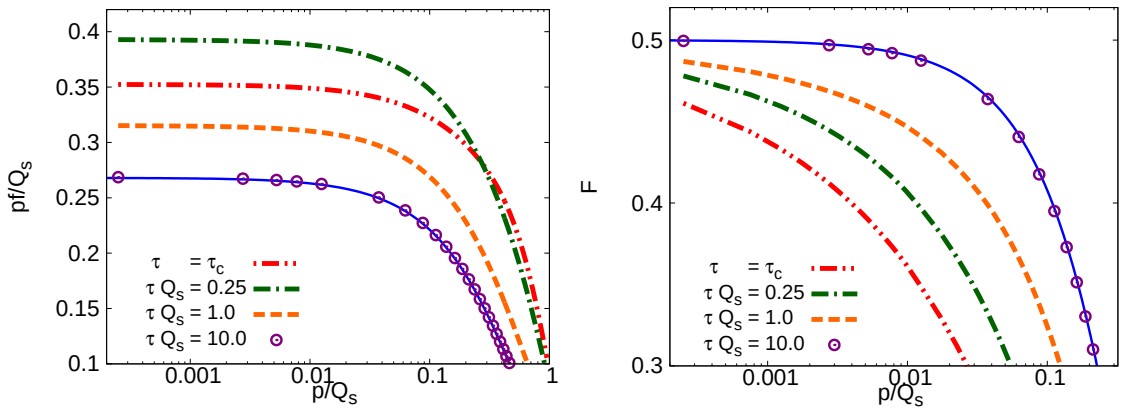

FIG. 9. Time evolution of pf and F after $\tau_c \simeq 0.1708\ Q_s^{-1}$. During $\tau_c \lesssim \tau \lesssim 0.25\ Q_s^{-1}$ the gluon distribution f increases at $p \lesssim Q_s$. After $\tau \simeq 0.25\ Q_s^{-1}$, f decreases to approach f_{eq}. In all the time F increases. At $\tau \simeq 10\ Q_s^{-1}$ f and F can be very well fitted by f_{eq} and F_{eq} with $\mu = 0$ and $T = 0.268\ Q_s$ (solid blue lines). Here, $f_0 = 0.4$ and $N_f = 3$.

is approximately given by

$$\frac{\partial}{\partial t} f \sim \alpha_s^2 N_c^2 f_0^2 (1 + f_0) \frac{Q_s^2}{p} - \alpha_s^2 \frac{N_f C_F f_0^2 Q_s^2}{2p} \tag{IV.51}$$

for $p \ll Q_s$, and p not too small. The first term on the right hand side of eq. (IV.51) is due to the second part of the current (II.7a), the part proportional to the integral $\mathcal{I}_b$, that drives the increase of the population of soft gluons. The second term is due to the quark production. It acts in the opposite direction, thus hindering the growth of soft gluon modes. However, as shown in Fig. 7, after a short transient period of time, the quark production is peaked at small momenta. This is also confirmed by the plot of the quark flux plotted in Fig. 8: the flux is the largest at small momenta, and continues to increase there all the way till the onset of BEC. In this regime, the quark production has no direct effect on the BEC itself. This is because, at small momenta, the outgoing quark current out of a small sphere of radius p_0 is compensated by the contribution to particle production in that small sphere (i.e. by the source term, as can be verified explicitly by using the small p expansions given in Appendix B, see in particular eq. (B.3)). This leaves only the gluon current produced by elastic collisions as the source of variation of particle number in the small sphere. And indeed the gluon flux displayed in Fig. 4 is very similar to that obtained for a purely gluonic system (see e.g. [3]).

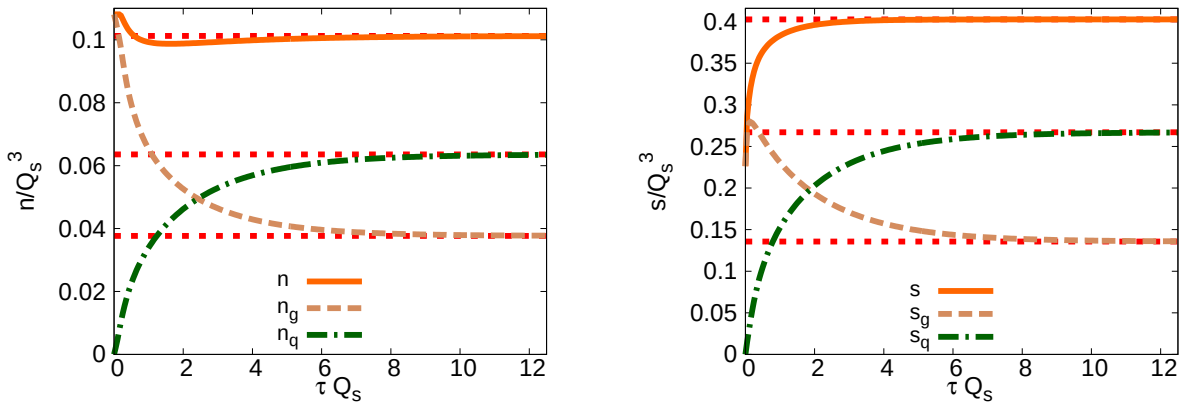

FIG. 10. Evolution of the number densities (left panel) and the entropy densities (right panel) of partons. The dotted red lines are the predicted values from thermodynamics. Here, $f_0 = 0.4$ and $N_f = 3$.

The thermal equilibration can be achieved only after the onset of gluon BEC. Fig. 9 shows how f and F evolve into thermal distributions after τ_c. As we mentioned above, the number of low momentum gluons keeps growing right after τ_c. This is a consequence of the relative small quark production rate (see Fig. 7) and the small formation rate of condensates $\dot{N}^0$ in comparison with the growth rate of low momentum gluons due to the collisions. In the meantime, $\dot{N}^0$ increases because of the increase of c_{-1} according to eq. (II.31). The occupation number of low momentum gluons stops growing and starts to decrease at a later time when the condensate formation rate and the quark production rate take over. Note that, as shown in Fig. 7, quark production takes place predominantly at low momentum. The high momentum quark modes are populated by transport. Afterwards, f keeps decreasing while F keeps increasing until the system achieves thermal equilibration. Fig. 10 shows the details about how the number and entropy densities evolve with τ and eventually reach the predicted values from thermodynamics in Sec. III.

At the end we shall discuss on what condition the quark production from gluons can be neglected. First, as we have shown in the case $f_0 \gtrsim 1$, τ_c is (almost) independent of N_f. On the other hand, for $f_0 \lesssim 1.0$ quark production delays the onset of BEC and τ_c increases as N_f increases. For example, for $f_0 = 0.4$ $\tau_c \simeq 0.14\ Q_s^{-1}$ with $N_f = 0$ and $\tau_c \simeq 0.1708\ Q_s^{-1}$ with $N_f = 3$. This can be easily understood from eq. (IV.46): the production of quarks and antiquarks contributes a negative term $\propto -\frac{N_f I_c(0)}{p} \bar{f}_0$ to $\bar{f}_1$, which obviously slows down the

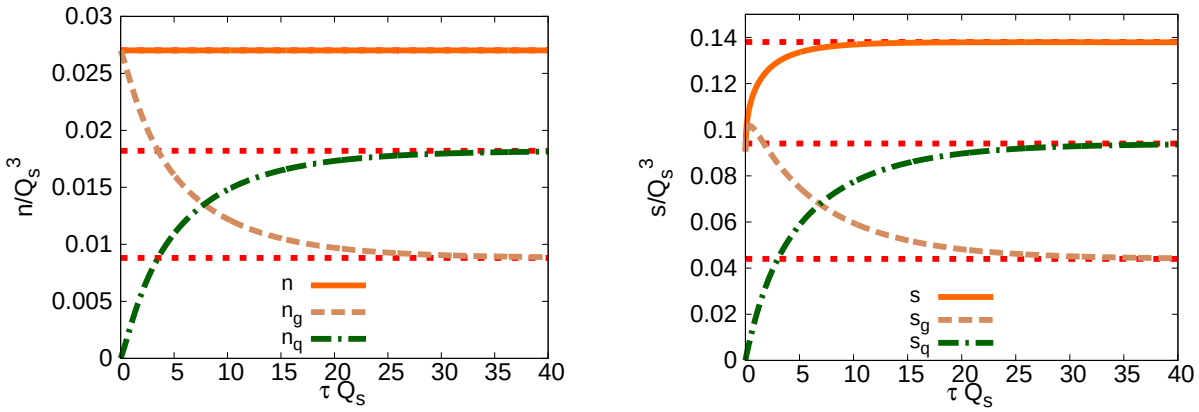

FIG. 11. Evolution of the number densities (left panel) and the entropy densities (right panel) of partons. The dotted red lines are the predicted values from thermodynamics. Here, $f_0 = 0.1$ and $N_f = 3$.

building-up of the $1/p$ tail of f if f_0 is not large enough. Second, we observe that the quark production itself slows down the approach to thermalization . To make this statement more quantitative, we define an equilibration time τ_{eq} by

$$\left|\frac{T^*(\tau_{eq})}{T} - 1\right| \leq 0.05, \quad \left|\frac{n_g(\tau_{eq})}{n_{geq}} - 1\right| \leq 0.05, \quad \left|\frac{n_q(\tau_{eq})}{n_{qeq}} - 1\right| \leq 0.05, \tag{IV.52}$$

and

$$\left|\frac{s_g(\tau_{eq})}{s_{geq}} - 1\right| \leq 0.05, \quad \left|\frac{s_q(\tau_{eq})}{s_{qeq}} - 1\right| \leq 0.05, \tag{IV.53}$$

where the values of the above quantities in thermal equilibrium are calculated using f_{eq} and F_{eq} with T and μ given by eq. (III.41). For $f_0 = 0.4$, we find $\tau_{eq} \simeq 1.1\ Q_s^{-1}$ with $N_f = 0$ and $\tau_{eq} \simeq 6.4\ Q_s^{-1}$ with $N_f = 3$. And for $f_0 = 1.0$, we find $\tau_{eq} \simeq 0.86\ Q_s^{-1}$ with $N_f = 0$ and $\tau_{eq} \simeq 4.8\ Q_s^{-1}$ with $N_f = 3$. Thus, the presence of quarks increases the thermalization time by typically a factor of 5 (for $N_f = 3$) (we should keep in mind however that this estimate suffers from the uncertainties related to our very approximate description of the dynamics beyond the onset of BEC).

B. Thermalization without BEC: $f_0 \leq f_{0t}$

For the initial distribution (III.38), with $f_0 \leq f_{0t}$, the quark-gluon system will achieve thermal equilibration without the formation of a BEC. Our numerical results verify that the

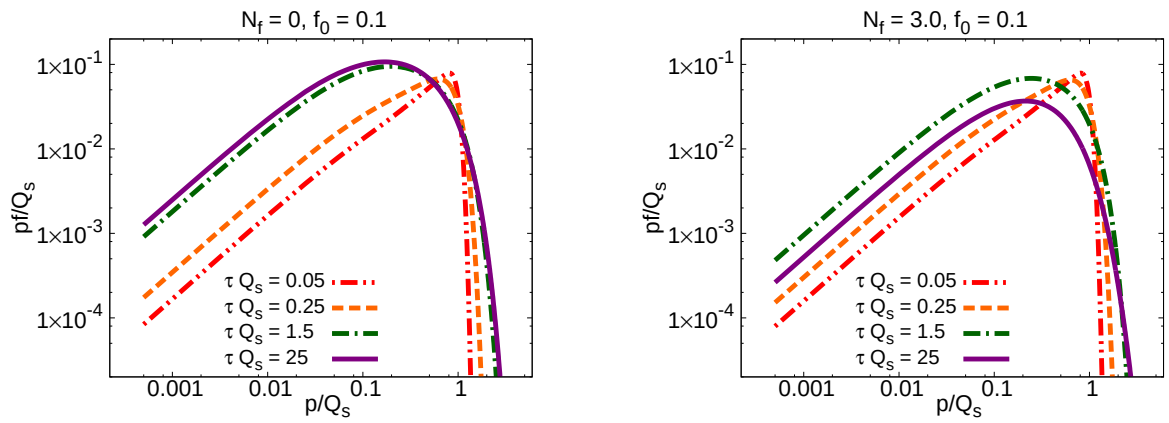

FIG. 12. The gluon distribution f for $N_f = 0$ and $N_f = 3$. In both cases, the solid curves at $\tau\ Q_s = 25$ are thermal equilibrium distributions. The left panel shows that for $N_f = 0$ the number of low momentum gluons continues to increase until the system achieves thermal equilibrium. The right panel shows that for $N_f = 3$ the number of low momentum gluons becomes larger than that in the thermal distribution far before the system thermalizes.

thermal equilibrium temperature T and the negative chemical potential μ are exactly those predicted by solving eq. (III.34). In those cases, the features of the thermalization process are qualitatively the same for all f_0. The quarks and antiquarks are produced from the the process $gg \to q\bar{q}$, which causes the gluon number to decrease keeping the total parton number constant. The entropy density of gluons becomes smaller at later times but the total entropy density always increases. Fig. 11 shows the details about how the number and entropy densities of the system with $f_0 = 0.1$ and $N_f = 3$ evolve into their predicted values in thermal equilibrium. These curves are quite similar to those in Fig. 10, with the noticeable difference that here the parton number n is exactly conserved.

With quark production being neglected, the system of gluons with $f_0 > f_{0c}|_{N_f=0} = 0.154$ thermalizes with the formation of BEC. As discussed in the previous subsection, the quark production contributes a term $\propto -N_f \frac{f_0^2}{p}\tau$ to f in the early time. For $f_{0t} > f_0 > f_{0c}|_{N_f=0} = 0.154$, this term is large enough to prevent f from building up the $1/p$ tail near $p = 0$, thereby inhibiting the formation of a BEC.

For the same f_0, the system with $N_f \geq 3$ has a lower equilibrium T and a smaller μ than that with $N_f = 0$, as shown in Fig. 2. Such a difference causes the under-populated system to thermalize in a different pattern. An example with $f_0 = 0.1$ is shown in Fig. 12. For

$N_f = 0$, the number of low momentum gluons continues to increase until the system achieves thermal equilibrium. For $N_f = 3$, the occupation number of gluons with $p \lesssim Q_s$ first reaches a maximum value which is higher than that in thermal equilibrium. Such an excess of gluons can not be tamed by the quark production until the late stages of equilibration. Let us define two effective chemical potentials

$$\mu_g^* \equiv -T^* \log\left(1 + \frac{1}{f(0)}\right), \qquad \mu_q^* \equiv -T^* \log\left(\frac{1}{F(0)} - 1\right), \tag{IV.54}$$

which are both equal to μ after the system thermalizes. If $f_0 < f_{0t}$, f near $p = 0$ can be approximated by f_{eq} with $\mu_g^*/T^* < 0$. Given f_0, one can determine the largest value of μ_g^*/T^* numerically. f_{0t} is defined by the value of f_0 for which the largest value of μ_g^*/T^* is zero. At the moment when $\mu_g^*/T^* = 0$, f looks like f_{eq} with a vanishing μ near $p = 0$. In the next subsection, we shall show that BEC can be formed due to such a transient excess of gluons in the system with $f_0 > f_{0t}$ and $N_f > 0$.

Like in the over-populated case, the quark production delays thermalization. The equilibration time τ_{eq} is redefined by replacing n_g/n_{geq} and n_q/n_{qeq} respectively by μ_g^*/μ and μ_q^*/μ in eq. (IV.52). In this definition, the first condition in eq. (IV.52) is a sufficient condition for f and F to be approximately equal to those in thermal equilibrium at small p while the second condition in eq. (IV.53) acts as a constraint to the shape of f and F for the full range of p. For $f_0 = 0.1$, we find $\tau_{eq} \simeq 5.5\ Q_s^{-1}$ with $N_f = 0$ and $\tau_{eq} \simeq 25\ Q_s^{-1}$ with $N_f = 3$ (again we observe that quark production delays the equilibration time by a factor of ~ 5).

C. Thermalization with transient BEC: $f_{0c} > f_0 > f_{0t}$

Transient BEC can be formed in the under-populated system with $f_0 > f_{0t}$. Let us take the system with $f_0 = 0.26$ and $N_f = 3$ as an example. As shown in the left panel of Fig. 13, f starts to become singular at $p = 0$ at $\tau_c = 0.947\ Q_s^{-1}$. At the moment, the gluon flux $\mathcal{F}_g$ still vanishes at $p = 0$ because the coefficient $c_{-1} = T^*$. However, c_{-1} has a tendency to increase due to the further accumulation of small momentum gluons. Like in the over-populated case, the solution to the transport equations exists after τ_c only if boundary conditions with a non-vanishing $\mathcal{F}_g|_{p=0}$ are provided. Using the boundary conditions in eq. (B.8) to solve the transport equations, we are able to follow the subsequent evolution of the system. $\mathcal{F}_g$ is found to become negative at $p = 0$ right after τ_c, which is shown in the right panel of

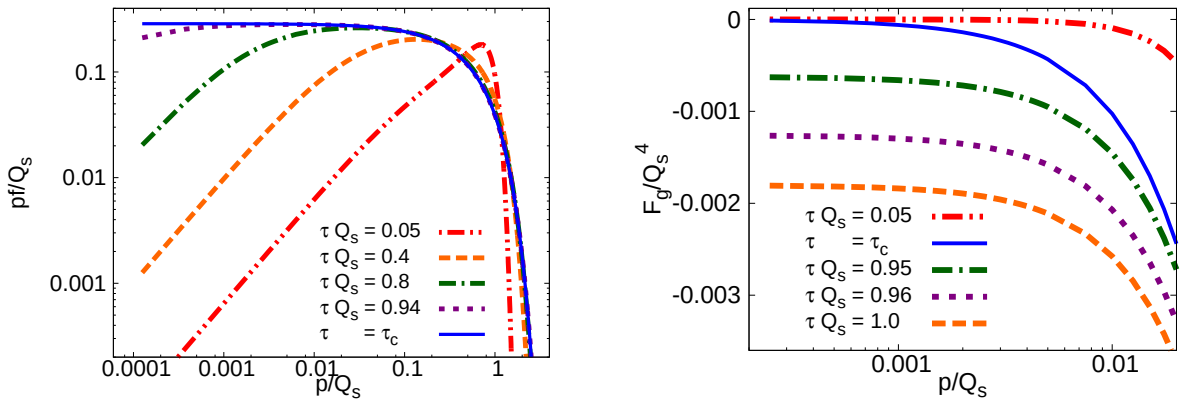

FIG. 13. Formation of transient BEC. The left panel shows the time evolution of pf as a function of p. The $1/p$ tail of f is built up at $\tau = \tau_c = 0.947\ Q_s^{-1}$. The right panel shows the small p behavior of the gluon flux $\mathcal{F}_g$ at different times. Right after τ_c, it becomes negative. Here, $N_f = 3$ and $f_{0t} < f_0 = 0.26 < f_{0c} = 0.308$.

Fig. 13. This indicates the formation of BEC and the number density of condensates can be calculated from the gluon flux at $p = 0$ according to eq. (II.31).

BEC can only exist for a short period of time since from thermodynamics the system is expected to eventually evolve into thermal equilibrium without BEC. As shown in the left panel of Fig. 14, n starts to decrease at $\tau = \tau_c$, which indicates the formation of BEC. However, n restores its original value after a period $\Delta\tau \simeq 0.35\ Q_s^{-1}$. Afterwards, the solution with vanishing $\mathcal{F}_g|_{p=0}$ exists again, which describes the subsequent evolution of the system. n does not change anymore and hence the condensates exist only for a time $\Delta\tau \simeq 0.35\ Q_s^{-1}$. As expected, f, as well as F, eventually becomes the thermal distribution, which is shown in the right panel of Fig. 14. For an even larger f_0, the transient BEC exists for a longer time. For example, we find that BEC starts to form at $\tau_c = 0.52\ Q_s^{-1}$ and exists for a period of $\Delta\tau \simeq 2.80\ Q_s^{-1}$ for $f_0 = 0.28$. In summary, the system with $f_{0c} > f_0 > f_{0t}$ serves as an example of thermalization with transient BEC.

V. DISCUSSIONS

In this paper we have studied the thermalization of a spatially homogeneous quark-gluon plasma, starting from an initial dense system of gluons. Two coupled transport equations

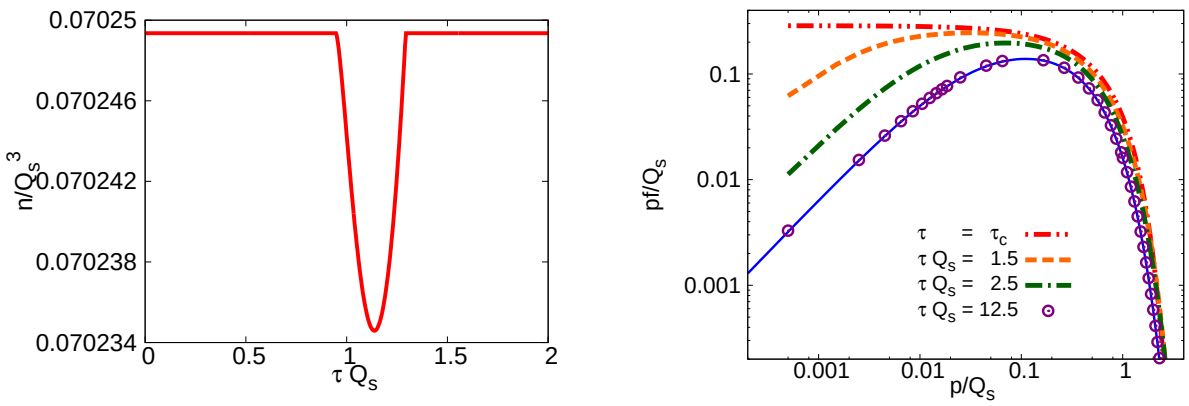

FIG. 14. Thermalization with transient BEC. The system with $f_0 = 0.26$ and $N_f = 3$ serves as an example of thermalization with transient BEC. Left panel shows n as a function of τ. BEC starts to be formed at $\tau_c = 0.947\ Q_s^{-1}$ but the condensates exist only in a short period $\Delta\tau \simeq 0.35\ Q_s^{-1}$. Right panel shows how the gluon distribution f evolves into a thermal distribution after $\tau = \tau_c$. The solid blue curve is the thermal distribution in eq. (III.33) with $T = 0.250\ Q_s$ and $\mu = -0.0357\ Q_s$.

for the gluon distribution f, and the quark distribution F, have been derived using the diffusion approximation of the Boltzmann equation, with the collision term accounting for all possible $2 \leftrightarrow 2$ scatterings between quarks and gluons. These transport equations are solved numerically to study how the system evolves from an initial gluon distribution $f_0\ \theta(1 - \frac{p}{Q_s})$ into a thermalized state of the quark-gluon plasma. We have studied systems with different values of f_0. N_f, the number of flavors of quarks that can be taken as massless, is also taken as a free parameter to study the influence of quark production on the formation of BEC and the equilibration process (more precisely, we compare the situation where $N_f = 3$ to that where $N_f = 0$). Our main conclusions are

- Quark production slows down the growth of f at $p \ll Q_s$.

  For $N_f = 0$, a BEC forms for $f_0 > f_{0c}|_{N_f=0} = 0.154$ in agreement with Ref. [3]. For finite N_f, there is a range of values of f_0 larger than $f_{0c}|_{N_f=0}$ for which quark production hinders the formation of a BEC, and for which the system thermalizes without the formation of a BEC. This occurs for $f_{0c} \leq f_0 \leq f_{0t}$, where f_{0t} depends on N_f. We find $f_{0t} \simeq 0.25937$ for $N_f = 3$.

- A transient BEC may develop in intermediate stages prior thermalization.

The critical value f_{0c} characterizing overpopulation depends on N_f. $f_{0c} = 0.308$ for $N_f = 3$. A BEC is not expected to be formed in equilibrium when $f_0 < f_{0c}$. However, we find that a transient BEC appears whenever $f_{0c} > f_0 > f_{0t}$. This is a consequence of the transient excess of low momentum gluons: the growth of low momentum gluon modes is a rapid process, while quark production is relatively much slower. The condensate only exists for a short period of time before quark production eventually takes over and suppresses the excess gluons as the system approaches thermal equilibration.

- In the regime of large overpopulation, i.e. for $f_0 \gtrsim 1$, the formation of BEC occurs at a finite time t_c given by the simple formula $t_c \sim \frac{1}{(\alpha_s f_0)^2}\frac{1}{Q_s}$. t_c is (almost) independent of N_f, that is, when f_0 is large enough, the onset of BEC is not affected by quark production.

- Quark production delays thermalization. The equilibration time, defined in eqs. (IV.52) and (IV.53), is typically about 5 to 6 times larger for $N_f = 3$ than that for $N_f = 0$.

There are several important issues that are not addressed in this paper. Like in Refs. [3, 9], we only focus on the thermalization of a spatially homogenous non-expanding system. The formation of BEC may also occur in the expanding quark-gluon system[2]. However, detailed (numerical) calculations are still missing in the literature, and it would be of great interest to extend the present work into, say, the boost-invariant 1+1 dimensional expanding system[6]. Moreover, the inelastic processes such as $2 \leftrightarrow 3$ are ignored in our transport equations, and it would be important to study how these modify the physical picture that emerges from the present calculation [4]. Besides, all the partons are taken as massless and like Ref. [3, 6, 7] the diffusion approximation is used to simplify the Boltzmann equation. The evolution of the condensates is simply described here by properly added boundary conditions. It would be important to check how reliable those approximations are by a more elaborated investigation on how the low momentum gluons evolve over time[10]. Finally, the validity of the kinetic description, although widely used in this type of problems, needs to be checked against the statistical classical field simulations, which may be more appropriate at early times [9, 11]. Comparison with the recent studies in Refs. [12, 13] would be particularly relevant. We leave all those interesting issues for future studies.

$ab \leftrightarrow cd$	$\lvert\mathcal{M}^{ab}_{cd}\rvert^2/g^4$	In diffusion approximation
$q_1q_2 \leftrightarrow q_1q_2$ $q_1\bar{q}_2 \leftrightarrow q_1\bar{q}_2$ $\bar{q}_1q_2 \leftrightarrow \bar{q}_1q_2$ $\bar{q}_1\bar{q}_2 \leftrightarrow \bar{q}_1\bar{q}_2$	$4N_cC_F\left(\frac{s^2+u^2}{t^2}\right)$	$8N_cC_F\frac{s^2}{t^2}$
$q_1q_1 \leftrightarrow q_1q_1$ $\bar{q}_1\bar{q}_1 \leftrightarrow \bar{q}_1\bar{q}_1$	$4N_cC_F\left(\frac{s^2+u^2}{t^2}+\frac{s^2+t^2}{u^2}\right)-8C_F\frac{s^2}{tu}$	$8N_cC_F\left(\frac{s^2}{t^2}+\frac{s^2}{u^2}\right)$
$q_1\bar{q}_1 \leftrightarrow q_1\bar{q}_1$	$4N_cC_F\left(\frac{s^2+u^2}{t^2}+\frac{t^2+u^2}{s^2}\right)-8C_F\frac{u^2}{st}$	$8N_cC_F\frac{s^2}{t^2}$
$q_1\bar{q}_1 \leftrightarrow q_2\bar{q}_2$	$4N_cC_F\left(\frac{t^2+u^2}{s^2}\right)$	0
$q_1\bar{q}_1 \leftrightarrow gg$	$8N_cC_F^2\left(\frac{u}{t}+\frac{t}{u}\right)-8N_c^2C_F\frac{t^2+u^2}{s^2}$	$-8N_cC_F^2\left(\frac{s}{t}+\frac{s}{u}\right)$
$q_1g \leftrightarrow q_1g$ $\bar{q}_1g \leftrightarrow \bar{q}_1g$	$-8N_cC_F^2\left(\frac{u}{s}+\frac{s}{u}\right)+8N_c^2C_F\frac{u^2+s^2}{t^2}$	$-8N_cC_F^2\frac{s}{u}+16N_c^2C_F\frac{s^2}{t^2}$
$gg \leftrightarrow gg$	$16N_c^2(N_c^2-1)\left(3-\frac{su}{t^2}-\frac{st}{u^2}-\frac{tu}{s^2}\right)$	$16N_c^2(N_c^2-1)\left(\frac{s^2}{t^2}+\frac{s^2}{u^2}\right)$

TABLE I. Squares of the $2 \leftrightarrow 2$ scattering amplitudes in QCD, with spins and colors of all four partons summed over. The dominant contributions of each process in diffusion approximation are given in the third column. The terms proportional to $\frac{s^2}{t^2}$ or $\frac{s^2}{u^2}$ contribute to the diffusion currents while the terms proportional to $\frac{s}{t}$ or $\frac{s}{u}$ only contribute to the source terms. Here, q_1 ($\bar{q}_1$) and q_2 ($\bar{q}_2$) represent quarks (antiquarks) of different flavors.

ACKNOWLEDGEMENTS

We would like to thank F. Gelis for many illuminating discussions. In addition, JPB thanks J. Liao and L. McLerran for collaboration that benefited this work. BW is supported by the Agence Nationale de la Recherche project # 11-BS04-015-01. The research of JPB and LY is supported by the European Research Council under the Advanced Investigator Grant ERC-AD-267258.

Appendix A: Diffusion approximation of the collision integral

In this appendix we simplify the collision term of the Boltzmann equation in eq. (II.3) within the diffusion approximation[5]. The squares of the amplitudes for all the $2 \leftrightarrow 2$

processes in QCD are listed in Table I. The momenta of the partons in the final state of these scattering processes are denoted respectively by K and K'. We only need to keep all the dominant contributions in the limit that the momentum transfer Q is much smaller than the momenta of the two scattering partons, which are denoted respectively by P and P'. Let us take the t channel dominated processes as an example, in which case $Q = K - P$. In the diffusion limit, the Mandelstam variables reduce to

$$s = (P + P')^2 = 2pp' - 2\mathbf{p}\cdot\mathbf{p}' = 2pp'(1 - \mathbf{v}\cdot\mathbf{v}'), \tag{A.1a}$$

$$t = Q^2 \simeq -q^2 + (\mathbf{q}\cdot\mathbf{v})^2, \tag{A.1b}$$

$$u = (P - K')^2 \simeq -2pp'(1 - \mathbf{v}\cdot\mathbf{v}') = -s \tag{A.1c}$$

with $\mathbf{v} \equiv \mathbf{p}/p$ and $\mathbf{v}' \equiv \mathbf{p}'/p'$, and

$$\delta(E_p + E_{p'} - E_k - E_{k'}) \simeq \delta(\mathbf{q}\cdot(\mathbf{v}' - \mathbf{v})). \tag{A.2}$$

The corresponding contributions from the u channel scattering can be obtained by simply interchanging K and K'. The leading contributions to $|\mathcal{M}^{ab}_{cd}|^2$ in the small angle approximation are given in the third column of Table I. By plugging the terms proportional to $\frac{s}{t}$ or $\frac{s}{u}$ into the collision term of eq. (II.3), one can easily obtain the source terms

$$\begin{aligned} S_g = -\frac{N_f}{C_F} S_q &= \frac{2\alpha_s^2 N_f C_F}{p}\left[F_{\mathbf{p}}(1+f_{\mathbf{p}}) - f_{\mathbf{p}}(1-F_{\mathbf{p}}))\right] \\ &\times \int \frac{d^3\mathbf{p}'}{(2\pi)^3}\frac{1}{p'}(f_{\mathbf{p}'} + F_{\mathbf{p}'}) \int d^3\mathbf{q} \frac{1 - \mathbf{v}\cdot\mathbf{v}'}{q^2 - (\mathbf{v}\cdot\mathbf{q})^2}\delta(\mathbf{q}\cdot(\mathbf{v}' - \mathbf{v})) \\ &= \frac{4\pi\alpha_s^2 \mathcal{L} C_F N_f \mathcal{I}_c}{p}\left[F_{\mathbf{p}}(1+f_{\mathbf{p}}) - f_{\mathbf{p}}(1-F_{\mathbf{p}})\right], \end{aligned} \tag{A.3}$$

where we have used the integral

$$\int d^3\mathbf{q}\left[\frac{1 - \mathbf{v}\cdot\mathbf{v}'}{q^2 - (\mathbf{q}\cdot\mathbf{v})^2}\right]\delta(\mathbf{q}\cdot(\mathbf{v} - \mathbf{v}')) = 2\pi\mathcal{L}. \tag{A.4}$$

The terms of $|\mathcal{M}^{ab}_{cd}|^2$ proportional to $\frac{s^2}{t^2}$ and $\frac{s^2}{u^2}$ in the limit $q \ll p, p'$ only contribute to the diffusion terms in the collision term of the transport equations. Let us write

$$\begin{aligned} \mathcal{C}[f^a_{\mathbf{p}}] =& \frac{1}{2p}\sum_{b,c,d}\int \frac{d^3\mathbf{p}'}{(2\pi)^3}\frac{d^3\mathbf{q}}{(2\pi)^3} w^{ab}_{cd}\left(\mathbf{p} + \frac{\mathbf{q}}{2}, \mathbf{p}' - \frac{\mathbf{q}}{2}, \mathbf{q}\right) \\ &\times \left[f^c_{|\mathbf{p}+\mathbf{q}|} f^d_{|\mathbf{p}'-\mathbf{q}|}(1+\epsilon_a f^a_{\mathbf{p}})(1+\epsilon_b f^b_{\mathbf{p}'}) - f^a_{\mathbf{p}} f^b_{\mathbf{p}'}(1+\epsilon_c f^c_{|\mathbf{p}+\mathbf{q}|})(1+\epsilon_d f^d_{|\mathbf{p}'-\mathbf{q}|})\right], \end{aligned} \tag{A.5}$$

where the relation of w^{ab}_{cd} to $|\mathcal{M}^{ab}_{cd}|^2$ can be obtained by referring to eq. (II.3), $\epsilon_i = 1$ for gluons and $\epsilon_i = -1$ for quarks and antiquark. To derive the diffusion terms of the transport

equations, one only needs to keep the terms in which the factors in the parentheses $[\cdots]$ on the right hand side of eq. (A.5) vanish in the limit $\mathbf{q} \to \mathbf{0}$. In this case, partons c and d can be respectively taken as the same species as a and b [‡]. Therefore, the diffusion terms describe the diffusion of particle a in the momentum space as a result of scattering off particle b. They are different from the source terms, which are proportional to the production rate of particle b of a different species from the scattering parton a with another parton. By expanding the integrand of eq. (A.5) in powers of q and keeping only the first non-vanishing term, we find, after some algebra,

$$\mathcal{C}_{diff}[f^a_{\mathbf{p}}] = -\nabla_{\mathbf{p}} \mathcal{J}^a, \tag{A.6}$$

where the diffusion current for particle a is given by

$$\begin{aligned} \mathcal{J}^{ai} \equiv & -\frac{1}{2p} \sum_b \int \frac{d^3\mathbf{p}'}{(2\pi)^3} \frac{d^3\mathbf{q}}{(2\pi)^3} \, w^{ab}_{diff}(\mathbf{p}, \mathbf{p}', \mathbf{q}) \\ & \times \frac{q^i q^j}{2} \left[f^b_{\mathbf{p}'}(1 + \epsilon_b f^b_{\mathbf{p}'}) \nabla_{p^j} f^a_{\mathbf{p}} - f^a_{\mathbf{p}}(1 + \epsilon_a f^a_{\mathbf{p}}) \nabla_{p'^j} f^b_{\mathbf{p}'} \right] \end{aligned} \tag{A.7}$$

with

$$w^{ab}_{diff}(\mathbf{p}, \mathbf{p}', \mathbf{q}) = \frac{1}{8pp'^2 \nu_a} 2\pi \delta(\vec{q} \cdot (\mathbf{v}' - \mathbf{v})) |\mathcal{M}^{ab}_{ab}|^2_{diff}. \tag{A.8}$$

Here, $|\mathcal{M}^{ab}_{ab}|^2_{diff}$ are the terms proportional to $\frac{s^2}{t^2}$ in the third column of Table I. To simplify $\mathcal{J}^a$, we need to evaluate

$$B^{ij} \equiv \int \frac{d^3\mathbf{q}}{(2\pi)^3} \frac{q^i q^j (1 - \mathbf{v} \cdot \mathbf{v}')^2}{[q^2 - (\mathbf{q} \cdot \mathbf{v})^2]^2} 2\pi \delta(\mathbf{q} \cdot (\mathbf{v} - \mathbf{v}')) \tag{A.9}$$

$$= \frac{\mathcal{L}}{4\pi} [\delta^{ij}(1 - \mathbf{v} \cdot \mathbf{v}') + (v^i v'^j - v'^i v^j)], \tag{A.10}$$

and

$$\begin{aligned} J^{ab} \equiv & -\frac{g^4}{8\nu_a} \nabla_{p^i} \int \frac{d^3\mathbf{p}'}{(2\pi)^3} B^{ij} \left[f^b_{\mathbf{p}'}(1 + \epsilon_b f^b_{\mathbf{p}'}) \nabla_{p^j} f^a_{\mathbf{p}} - f^a_{\mathbf{p}}(1 + \epsilon_a f^a_{\mathbf{p}}) \nabla_{p'^j} f^b_{\mathbf{p}'} \right] \\ = & -\frac{\pi \alpha_s^2 \mathcal{L}}{2\nu_a} \nabla_{\mathbf{p}} \cdot \int \frac{d^3\mathbf{p}'}{(2\pi)^3} \left[f^b_{\mathbf{p}'}(1 + \epsilon_b f^b_{\mathbf{p}'}) \nabla_{\mathbf{p}} f^a_{\mathbf{p}} + \frac{2 f^b_{\mathbf{p}'}}{p'} f^a_{\mathbf{p}}(1 + \epsilon_a f^a_{\mathbf{p}}) \mathbf{v} \right]. \end{aligned} \tag{A.11}$$

Here, we have assumed that $f^b_{\mathbf{p}} = f^b_{-\mathbf{p}}$ in order to get J^{ab} in the last line in the above equation. $\mathcal{J}^a$ in eq. (II.7) is obtained by summing J^{ab} over b with the coefficient given by that of the corresponding term proportional to $\frac{s^2}{t^2}$ in the third column of Table I.

[‡] Here, we need only to consider the dominant terms from the t channels. There are equal contributions from the u channels if particles c and d are identical particles. However, the sum of the contributions from both channels should be divided by 2.

Appendix B: Series solutions and boundary conditions to the transport equations

As discussed in the main text, there are two types of solutions of the transport equations, characterized by the behavior of the gluon distribution near the origin $p = 0$: either $f(p = 0)$ is a finite constant, or $f(p \to 0) \sim 1/p$. In order to analyze further these solutions, we set

$$f = \sum_n c_n p^n, \qquad F = \sum_n d_n p^n \tag{B.1}$$

where the coefficients c_n and d_n can be determined from the transport equations in eqs. (II.12) and (II.13) with I_a, I_b and I_c taken as functions only of τ. One then finds that there are only two types of solutions allowed by the transport equations:

- f is analytic at $p = 0$.

  In this case, we have

$$\begin{aligned} f &= c_0 + \frac{C_F N_f I_c[c_0 - (2c_0+1)d_0] - 2N_c c_0(c_0+1)I_b}{2N_c I_a} p + O(p^2), \\ F &= d_0 + \frac{C_F I_c[c_0(2d_0-1) + d_0] + 2(d_0-1)d_0 I_b}{2I_a} p + O(p^2), \end{aligned} \tag{B.2}$$

  and

$$\begin{aligned} -J_g &= -\frac{C_F N_f I_c[c_0(2d_0-1)+d_0]}{2N_c} + O(p), \\ -J_q &= \frac{1}{2} C_F I_c[c_0(2d_0-1)+d_0] + O(p) \end{aligned} \tag{B.3}$$

  with $c_0 = f(\tau, 0)$ and $d_0 = F(\tau, 0)$.

  In the limit $c_0 \gg 1$, the radius of convergence of the above series solution shrinks to zero. In this case, we find

$$f = c_0 + \left[-c_0^2 + O(c_0)\right] \frac{p}{T^*} + \left[c_0^3 + O(c_0^2)\right] \left(\frac{p}{T^*}\right)^2 + \cdots, \tag{B.4}$$

  with $T^* \equiv \frac{I_a}{I_b}$. The leading terms in c_0 at each order in p can be resummed and, thus, we obtain

$$f \simeq \frac{c_0}{1 + \frac{c_0 p}{T^*}} = \frac{T^*}{p - \mu_g^*} \tag{B.5}$$

  with the effective chemical potential $\mu_g^* \equiv -T^*/c_0$. The above resummed solution is very useful for understanding the evolution of the quark-gluon system close to τ_c[3].

- f is singular at $p = 0$.

  In this case, we get

$$f = \frac{c_{-1}}{p} - \frac{1}{2} + \frac{I_a\left[-C_F N_f I_c + 2N_c\dot{c}_{-1} + N_c I_b\right] + C_F c_{-1} I_c\left[I_b(N_f - N_c) - 2N_c\dot{c}_{-1}\right]}{4N_c(2c_{-1}I_b + I_a)(I_a - C_F c_{-1} I_c)} p + O(p^2),$$
$$F = \frac{1}{2} + \frac{I_b - C_F I_c}{4(C_F c_{-1} I_c - I_a)} p + O(p^3), \tag{B.6}$$

  and

$$-J_g = \frac{c_{-1}(c_{-1}I_b - I_a)}{p^2} + \frac{1}{4}\left(\frac{C_F N_f I_c(I_a - c_{-1}I_b)}{N_c(C_F c_{-1} I_c - I_a)} + 2\dot{c}_{-1}\right) + O(p^2),$$
$$-J_q = \frac{C_F I_c(I_a - c_{-1}I_b)}{4(I_a - C_F c_{-1} I_c)} + O(p^2). \tag{B.7}$$

To solve the transport equations in eqs. (II.12) and (II.13), one needs two initial conditions and four boundary conditions. In our code, we use the following boundary conditions

$$\mathcal{F}_g|_{p=\infty} = 0, \quad \mathcal{F}_g|_{p=0} = 4\pi c_{-1}\left(I_a - I_b c_{-1}\right), \quad \mathcal{F}_q|_{p=\infty} = 0, \quad \mathcal{F}_q|_{p=0} = 0. \tag{B.8}$$

The explicit Euler method is used for time integration and only c_{-1} at the current time step is needed for the calculation of f and F at the next time step.

---

[1] A. H. Mueller, Nucl. Phys. B **572**, 227 (2000) [hep-ph/9906322].

[2] J. -P. Blaizot, F. Gelis, J. -F. Liao, L. McLerran and R. Venugopalan, Nucl. Phys. A **873**, 68 (2012) [arXiv:1107.5296 [hep-ph]].

[3] J. -P. Blaizot, J. Liao and L. McLerran, Nucl. Phys. A **920**, 58 (2013) [arXiv:1305.2119 [hep-ph]].

[4] X. -G. Huang and J. Liao, arXiv:1303.7214 [nucl-th].

[5] L. P. Pitaevskii and E.M. Lifshitz, "Physical Kinetics," Pergamon Press (1981).

[6] A. H. Mueller, Phys. Lett. B **475**, 220 (2000) [hep-ph/9909388].

[7] J. Bjoraker and R. Venugopalan, Phys. Rev. C **63**, 024609 (2001) [hep-ph/0008294].

[8] P. B. Arnold, G. D. Moore and L. G. Yaffe, JHEP **0301**, 030 (2003) [hep-ph/0209353].

[9] T. Epelbaum and F. Gelis, Nucl. Phys. A **872**, 210 (2011) [arXiv:1107.0668 [hep-ph]].

[10] J. -P. Blaizot, J. Liao and L. McLerran, in progress.

[11] A. H. Mueller and D. T. Son, Phys. Lett. B **582**, 279 (2004) [hep-ph/0212198].

[12] J. Berges, K. Boguslavski, S. Schlichting and R. Venugopalan, arXiv:1303.5650 [hep-ph].

[13] T. Epelbaum and F. Gelis, Phys. Rev. Lett. **111**, 232301 (2013) [arXiv:1307.2214 [hep-ph], arXiv:1307.2214 [hep-ph]].